Fluid Dynamics & Materials Processing

Tech Science Press

DOI: 10.32604/fdmp.2023.041852

ARTICLE

Gas-Water Production of a Continental Tight-Sandstone Gas Reservoir under Different Fracturing Conditions

Yan Liu[1], Tianli Sun[2], Bencheng Wang[1,*] and Yan Feng[2]

[1]Southwest Oil and Gas Company, SINOPEC, Chengdu, 610041, China

[2]The Second Gas Production Plant of Southwest Branch, SINOPEC, Nanchong, 637455, China

[*]Corresponding Author: Bencheng Wang. Email: wangbenc1@163.com

Received: 08 May 2023 Accepted: 14 July 2023 Published: 27 June 2024

ABSTRACT

A numerical model of hydraulic fracture propagation is introduced for a representative reservoir (Yuanba continental tight sandstone gas reservoir in Northeast Sichuan). Different parameters are considered, i.e., the interlayer stress difference, the fracturing discharge rate and the fracturing fluid viscosity. The results show that these factors affect the gas and water production by influencing the fracture size. The interlayer stress difference can effectively control the fracture height. The greater the stress difference, the smaller the dimensionless reconstruction volume of the reservoir, while the flowback rate and gas production are lower. A large displacement fracturing construction increases the fracture-forming efficiency and expands the fracture size. The larger the displacement of fracturing construction, the larger the dimensionless reconstruction volume of the reservoir, and the higher the fracture-forming efficiency of fracturing fluid, the flowback rate, and the gas production. Low viscosity fracturing fluid is suitable for long fractures, while high viscosity fracturing fluid is suitable for wide fractures. With an increase in the fracturing fluid viscosity, the dimensionless reconstruction volume and flowback rate of the reservoir display a non-monotonic behavior, however, their changes are relatively small.

KEYWORDS

Tight sandstone gas reservoir; fracture propagation; flowback rate; gas production law; water production law; influencing factor

1 Introduction

With the deepening of oil and gas exploration, the development of unconventional oil and gas resources has been attached equal importance to that of conventional oil and gas resources [1–4]. The world's unconventional oil and gas recoverable resources are 5833.5×10^8 t, of which unconventional oil is 4209.4×10^8 t (accounting for 72.2%), and unconventional natural gas is 195.4×10^{12} m^3 (accounting for 27.8%) (Fig. 1). Under the circumstances of shortage of conventional oil and gas resources and increasing contradiction between supply and demand, unconventional oil and gas resources are abundant and have become an effective supplement to conventional oil and gas resources. Under this circumstance, accelerating the rational and efficient development of tight gas is of great significance to ensure national energy security [5–12]. Unconventional oil and gas resources in Sichuan Province have currently been fully researched and extensively developed, among which the development of continental tight sandstone

reservoir is particularly important, which is rapidly becoming the third pole of growth besides Marine carbonate conventional gas and Marine shale gas, and is an important part of increasing oil and gas reserves and production now and future [3–18].

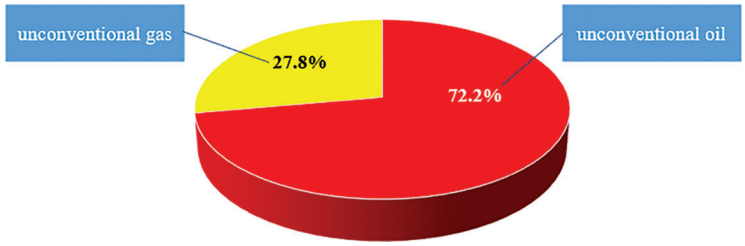

Figure 1: Proportion of geological reserves of unconventional oil and gas resources

Generally, tight sandstone gas reservoirs have strong reservoir heterogeneity. Hydraulic fractures tend to cross zones during fracturing and excessive vertical propagation of fractures leads to extra energy loss, which will make it hard for fractures to extend horizontally in the target zone effectively (Fig. 2) [19–28]. Under the condition of strong heterogeneous layer, the fracture propagation behavior of hydraulic fracturing not only depends on the characteristics of the target layer, but also is closely related to the mechanical properties of the upper and lower spacers. Thereby, it is considered that the stress difference between the target layer and the upper and lower spacers [29,30], the viscosity of fracturing fluid [31], and the fracturing displacement [32] are the relevant factors affecting vertical fracture propagation. However, the correlation among them has not been fully clarified [33–36]. In this article, a numerical fracture propagation model is established to study the hydraulic fracture propagation law of deep tight sandstone under different interlayer stress difference, fracturing construction displacement and fracturing fluid viscosity on the basis of comprehensive analysis of the geological characteristics, development status and low efficiency of stimulation and reconstruction of low permeability reservoir in Northeast Sichuan. Combined with reservoir numerical simulation, this paper analyzed the law of backflow, water production and gas production of tight sandstone gas reservoirs under different influencing factors, defined the fracture initiation and extension modes of continental reservoirs, aimed to establish a reasonable backflow process system to improve the reservoir reconstruction and stimulation potential of target blocks.

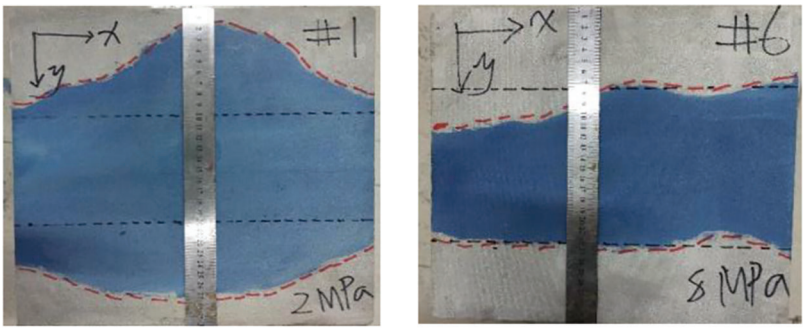

(a) Channeling (b) Not channeled

Figure 2: Fracture vertical expansion under different conditions

2 Typical Reservoir Characteristics

The gas reservoir A in Yuanba area in Northeast Sichuan Province is a typical deep continental tight sandstone gas reservoir of China. The average completion depth of reservoir A is 5 km, with more than 6 km of maximum burial depth, 1.99% average porosity and 0.069 mD average permeability. Its reservoir porosity and permeability are very low, and it is a typical ultra-low porosity and permeability reservoir [37–39]. The reservoir rock types are diverse, which can be divided into conglomerate, sandy conglomerate, calcareous sandstone, conventional sandstone, siltstone, etc., among which carbonate lithic conglomerate takes up the main part of them (Fig. 3), with micro-pore——micro-roar type of pore throat type and poor structure. The whole reservoir is based on a small quantity of poor gas layer and gas bearing layer. Vertically, the gas reservoir mainly develops I + II + III sand group, and 1–3 reservoirs are developed in the single sand group. The thickness of single layer reservoir is relatively thin (0.25–10 m, with an average of 3.5 m), and the reservoir is generally characterized by fractured and fractures-pore gas reservoirs. The reservoir space mainly includes the following five types: inter-granular dissolution pores, inter-granular-inter-granular dissolution micro-pores, clay minerals and dolomite inter-granular dissolution pores, limestone caves and fractures [40–42]. Most gas wells in this area have low production, rapid decrement and poor development effect. In general, the productivity of gas reservoir A in Yuanba area of Northeast Sichuan Province is mainly controlled by favorable lithology (calcarenaceous sandstone, sandy conglomerate), reservoir thickness and fractures. The larger the reservoir thickness, the more developed the fractures and the higher the productivity.

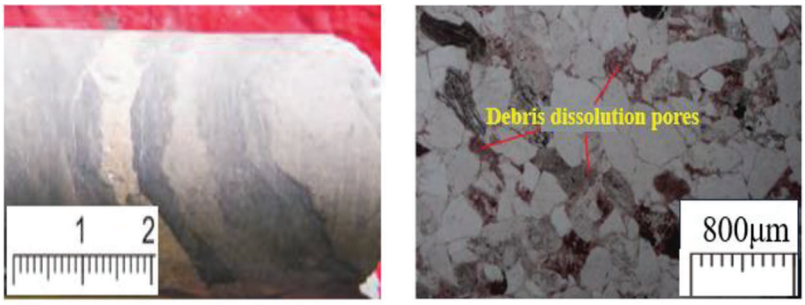

(a) Tight sandstone cores (b) Pore types

Figure 3: Cores and pore types of tight sand stones

3 Numerical Modeling and Verification

A numerical model of hydraulic fracture propagation was established based on the Discrete Fracture Network (DFN) model, which combined with fractured reservoir geology enabled hydraulically induced discrete fractures to initiate and extend vertical and horizontal fractures across three principal planes. The discrete fracture network can be solved based on continuity equation, mass conservation equation, constitutive relation and momentum equation [43–47].

continuity equation:

$$q_i = \frac{\partial V_{fi}}{\partial t} + \frac{\partial V_{li}}{\partial t} + \sum_{j=1}^{N} \frac{\partial V_{ji}}{\partial t} \tag{1}$$

mass conservation equation:

$$\int_0^t q(\tau)d\tau - V_l(t) - V_{sp}(t) = V_f(t) \tag{2}$$

DFN momentum equation:

$$\frac{dp}{d\zeta} = -\frac{f}{2}\frac{\rho\langle\bar{v}\rangle^2}{d_h} \tag{3}$$

laminar flow:

$$\frac{dp}{dx} = -\left(\frac{2n'+1}{4n'}\right)^{n'}\frac{k'(q/a)^{n'}}{\Phi(n')^{n'}b^{2n'+1}} \tag{4}$$

turbulent flow:

$$\frac{dp}{dx} = -\frac{f}{2}\frac{\rho q^2}{\pi^3 a^2 b^3} \tag{5}$$

width-opening pressure constitutive relationship:

$$w_\zeta = \Gamma_w\frac{2H_\zeta(p_\zeta - \sigma_\zeta - \Delta\sigma_{\zeta\zeta})}{E'} \tag{6}$$

where q is the flow rate of discrete fractures, V_l is fluid loss volume, V_f is fracture volume, V_{sp} is volume loss by spurt, t is time, N is total number of transverse fractures, p is pressure, f is Dracy friction factor, ρ is density of fracturing fluid, $\bar{v}$ is the cross-sectional average flow velocity, d_h is hydraulic diameter, a is ellipse major axis, b is ellipse minor axis, k' is consistency index, n' is flow behavior index, Φ is fluid loss parameter, ζ is dimensionless coordinate, w is fracture width, Γ is generalized influence function, H_ζ is characteristic fracture half-dimension, p_ζ is fracture pressure, σ_ζ is confining pressure, $\Delta\sigma_{\zeta\zeta}$ is fracture induced stress field along the ζ-axis, E' is effective Young's modulus.

In this article, a numerical model of hydraulic fracturing fracture propagation for gas wells in gas reservoir A of Yuanba area in Northeast Sichuan Province is established [48,49], and the numerical simulation of hydraulic fracture size and fracturing construction pressure is carried out for the target strata according to the actual pumping procedure of sand fracturing on site. The basic parameters of the model can be seen in Table 1. After fracturing, the fracture length, width and height of the first member of the target formation are respectively 178 m, 4.4 mm and 43 m. The comparison curve between the simulated pressure and the actual pressure is shown in Fig. 4, which demonstrates that the curves of simulated pressure and actual pressure are basically consistent with each other. This model has high accuracy and is in line with the actual situation on site, therefore it can be used to carry out the study on numerical simulation of influencing factors of hydraulic fracture propagation in target areas.

Table 1: Length, width and height of fracture under different interlayer stress difference conditions

Stress (MPa)	Fracture length (m)	Fracture width (cm)	Fracture height (m)
1	138.85	0.408	93.643
2	135.52	0.372	61.427
4	178.95	0.445	43.009
6	204.57	0.477	34.967
8	213.89	0.489	32.511
10	218.86	0.496	31.337

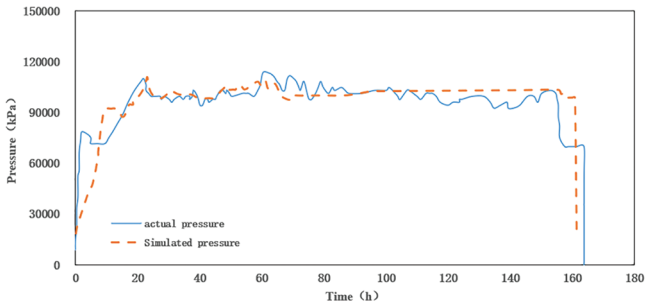

Figure 4: Comparison curve between simulated pressure and actual pressure

4 Fracture Propagation Rule under Different Influencing Factors

According to literature research, the importance of different parameters on hydraulic fracture propagation is ranked as: inter-layer stress difference > displacement > reservoir thickness > Young's modulus heterogeneity > fracturing fluid viscosity > permeability heterogeneity, among which inter-layer stress difference, fracturing fluid displacement and reservoir thickness are significantly related to fracture geometry [29–32]. Combined with the actual situation on site and considering the feasibility of fracturing construction, this article selects three influencing factors: (1) inter-layer stress difference, (2) fracturing construction displacement and (3) fracturing fluid viscosity to study the law of hydraulic fracture propagation under different influencing factors in the study area, using the control variable method and the numerical model of hydraulic fracturing fracture propagation.

4.1 Inter-Layer Stress Difference

Under complex geological conditions, the propagation of hydraulic fracture network not only depends on the characteristics of the target layer, but also is closely related to the mechanical properties of the upper and lower spacers. The stress difference between the target layer and the upper and lower spacers is an important factor which affects the vertical propagation of fractures. When the stress difference between the inter-layer is too small, the fracture is easy to channel the layer in the fracturing process, resulting in vertical fractures and energy loss. As a result, it is difficult to extend the fracture in the horizontal section of the target layer. According to the actual geological conditions in the Northeast Sichuan area, six hydraulic fracturing numerical simulations are carried out with the stress difference of inter-layer being 1, 2, 4, 6, 8 and 10 MPa.

Table 2 shows the fracture length, width and height of different inter-layer stress differences while Fig. 5 demonstrates the dimensionless reconstruction volume curves. The numerical simulation results show that the fracture length and width of gas reservoir A in Yuanba area of Northeast Sichuan Province are positively related to the stress difference of inter-layer while the fracture height decreases significantly with the increase of the stress difference of the inter-layer, showing a negative correlation with the inter-layer stress difference. At the same time, a negative correlation is shown between the stimulation volume and the stress difference of the inter-layer. With the increase of stress difference, the change rate of fracture geometric dimension decreases gradually. When the stress difference is greater than 6 MPa, the change rate of the fracture geometric dimension decreases significantly, and the variation range of the fracture length, width and height per unit stress difference of the interlayer has a significant reduction, which indicates that the expansion of hydraulic fracture can be effectively restricted when the stress difference of the inter-layer increases to a certain range.

Table 2: Length, width and height of fractures under different fracturing displacement conditions

Construction displacement (m^3/min)	Fracture length (m)	Fracture width (cm)	Fracture height (m)
2	177.49	0.329	35.825
4	182.09	0.329	40.243
8.5	187.19	0.338	43.009
12	187.38	0.349	43.376
15	187.97	0.357	43.531
20	189.04	0.365	43.545

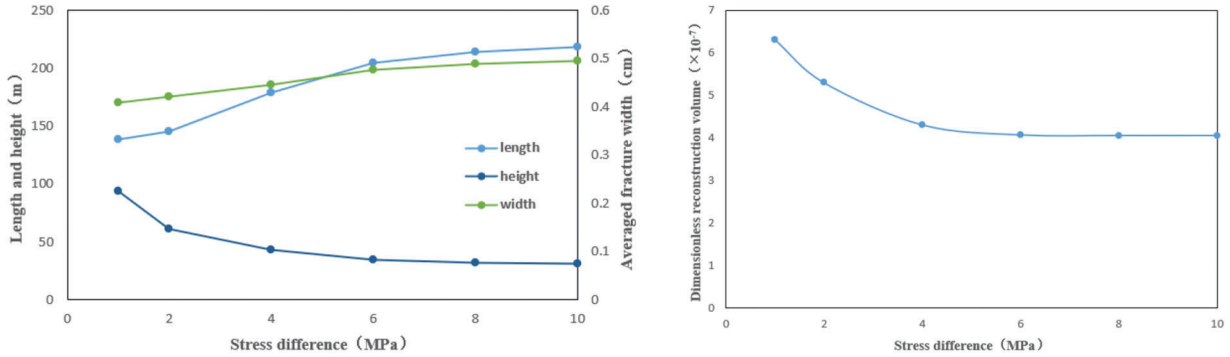

(a) Fracture size

(b) Reservoir dimensionless reconstruction volume

Figure 5: Fracture size and dimensionless reconstruction volume curves under different inter-layer stress differences

4.2 Fracturing Construction Displacement

The pumping displacement of fracturing fluid during construction has a significant influence on the expansion form of fracture network. The fractures *jumping up and down* can be controlled by restricting the construction displacement to realize the deep penetration of artificial fractures in low permeability tight reservoir. At the same time, as a crucial controlling factor affecting the propagation of hydraulic fractures, fracturing construction displacement can be flexibly adjusted according to the fracturing construction situation, which is a feasible method to control the geometric dimension of fractures. Combined with the actual geological and engineering conditions, the hydraulic fracturing numerical simulation is carried out in six different conditions with the fracturing construction displacement of 2, 4, 8.5, 12, 15 and 20 m^3/min.

Table 2 and Fig. 6 respectively show the fracture length, width, height and dimensionless reconstruction volume curves of fractures under different fracturing construction displacement conditions. The numerical simulation results show that the fracture length, width and height are positively related to the fracturing construction displacement. The larger the construction displacement is, the longer the hydraulic fracture, the wider the fracture, and the larger the fracture height is. Large displacement fracturing work can expand the fracture size and effectively increase the fracture reconstruction volume, and the variation range of fracture geometry dimension under different fracturing displacement is smaller than that under different inter-layer stress difference. Further more, when the construction displacement is greater than 8.5 m^3/min, the growth rate of fracture size slows down and the fracturing efficiency decreases. Considering the fracturing construction cost and reservoir reconstruction volume, the construction displacement should be roughly set at 8.5 m^3/min.

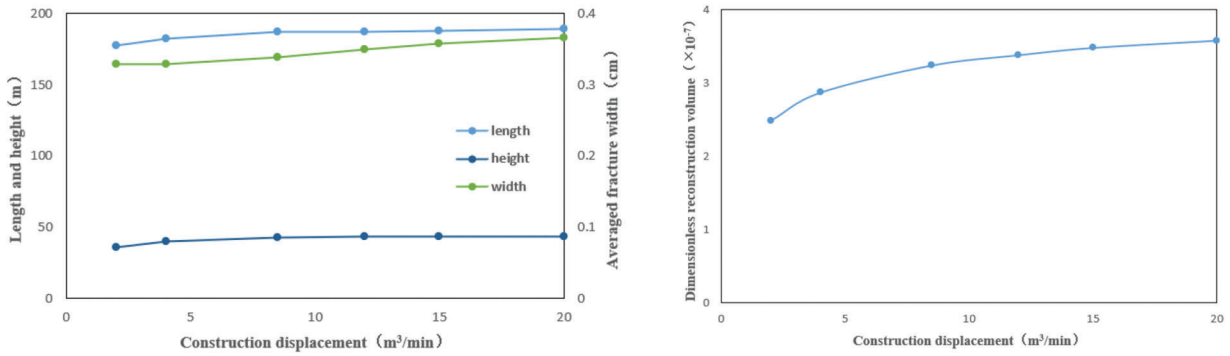

(a) Fracture size

(b) Reservoir dimensionless reconstruction volume

Figure 6: Fracture size and dimensionless reconstruction volume curves under different fracturing construction displacements

4.3 Fracturing Fluid Viscosity

The technological parameters and rheological properties of fracturing fluid have an important influence on the construction effect of hydraulic fracturing. With other conditions invariant, the higher the viscosity of fracturing fluid, the wider the fracture. When the fracture volume is invariant, the fracture length is shorter while the fracturing fluid viscosity is higher. Reasonable selection of fracturing fluid viscosity plays a decisive role in the successful reconstruction of reservoir. Combined with the types and rheological parameters of fracturing fluids used in the actual fracturing process in Yuanba area, five kinds of hydraulic fracturing numerical simulations with levels of 100, 300, 500, 800 and 1000 mPa·s of fracturing fluids viscosity are set.

Table 3 and Fig. 7 show the fracture length, width, height and dimensionless fracture reconstruction volume curves under different fracturing fluid viscosity. The numerical simulation results show that the fracture length is inversely proportional to the fracturing fluid viscosity, and the fracture width and height are proportional to the fracturing fluid viscosity. When the fracturing fluid viscosity increases from 100 to 1000 mPa·s, the fracture width and height increase significantly, while the fracture length has an obvious decrease. The fracture length, width and height showed strong sensitivity to the fracturing fluid viscosity. The fracture size varied widely with the change of fracturing fluid viscosity, and the dimensionless fracturing volume changes little. The fracture length after hydraulic fracturing with low viscosity is relatively long while the width and height of the fracture are relatively low, which is suitable for making long fractures. Fracturing with high viscosity makes fractures with short fracture length and relatively high fracture height and the fracture width, which is suitable for making wide fractures. With 500 mPa·s as the limit, too high or too low fracturing fluid viscosity will reduce the dimensionless reconstruction volume of hydraulically fractured reservoir.

Table 3: Length, width and height of fractures under different fracturing fluid viscosity conditions

Fluid viscosity (mPa·s)	Fracture length (m)	Fracture width (cm)	Fracture height (m)
100	348.68	0.239	34.69
300	271.66	0.311	36.911
500	223.71	0.369	39.79
800	178.95	0.445	43.01
1000	146.7	0.527	45.77

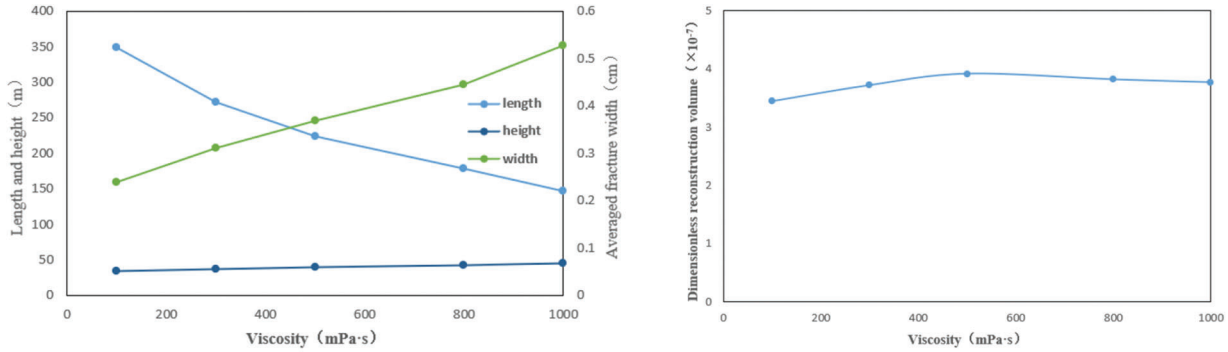

(a) Fracture size (b) Reservoir dimensionless reconstruction volume

Figure 7: Fracture size and dimensionless reconstruction volume curves under different fracturing fluid viscosity

5 Flow-Back Law and Flow-Back System

Increasing fracturing fluid flow-back rate can reduce the damage on fracture wall and formation, and reduce fresh water consumption in fracturing. As an important index to evaluate fracturing effect, fracturing fluid flow-back rate is directly related to the production of fractured reservoir [50,51]. By establishing the geological model around the well, the flow-back law of fracturing fluid under different influencing factors and different flow-back system is studied.

Fig. 8 shows the flow-back rate of fracturing fluid under different inter-layer stress difference, different fracturing construction displacement and different fracturing fluid viscosity. The simulation results show that the flow-back rate of fracturing fluid in Yuanba A gas reservoir is negatively correlated with the inter-layer stress difference, and positively correlated with the fracturing displacement. With the increase of fracturing fluid viscosity, the flow-back rate increases at first and then decreases. The pattern is basically consistent with the trend of dimensionless reconstruction volume influence. This is because with the increase of inter-layer stress difference and the decrease of fracturing displacement, the fracturing fluid formation intrusion increases, the volume of fracturing fluid used for fracture-building decreases, and the dimensionless fracture reconstruction volume decreases, which ultimately leads to the decrease of the fracturing fluid flow-back rate. The fracture flow-back rate reaches the highest level when the fracturing fluid viscosity is around 500 mPa·s. Additionally, under the same construction scale, increasing fracturing displacement can effectively reduce fracturing operation time and formation intrusion.

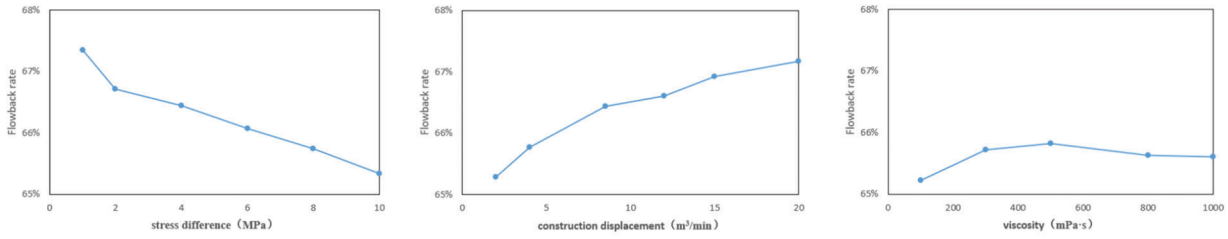

(a) Interlayer stress difference (b) Fracturing construction displacement (c) Fracturing fluid viscosity

Figure 8: Fracturing fluid flow-back rate curves under various influencing factors

6 Research on Productivity and Water Production Law

After historical fitting to ensure the accuracy of the established numerical reservoir model of gas reservoir A in Yuanba area in Northeast Sichuan, the characteristic well H in the target block is selected to carry out the study on the gas and water production law after single well pressure. In this article, the rectangular reservoir with 700 m × 300 m × 400 m I × J × K including well H was intercepted as the study area, the longitudinal grid step size was divided according to the thickness of small beds, and the fractures were preset according to the numerical simulation results of fracture propagation (Fig. 9). The reservoir physical property parameters and fluid physical property parameters in the study area were set according to the indoor core statistical data (Table 4). There is a vertical well in the middle of the study area, through which hydraulic fracturing and production law of pressurized gas and water can be studied.

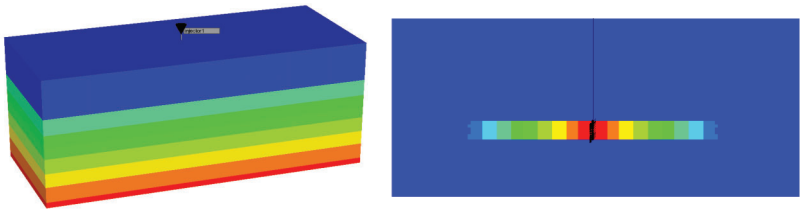

(a) Geological model around wells in the study area

(b) Preset fracture diagram

Figure 9: Geological model of the study area and schematic diagram of preset fracture distribution

Table 4: Main parameter of model

Parameter	Value	Parameter	Value	Parameter	Value
Reservoir pressure (MPa)	89.27	Reservoir temperature (K)	343.15	Reservoir size (m × m)	700 × 300
Target layer thickness (m)	61	Water saturation	0.24~0.71	Young's modulus (GPa)	28~80
Matrix porosity	0.027~0.084	Matrix permeability (mD)	0.01~0.093	Poisson's ratio (dimensionless)	0.17~0.32

6.1 Inter-Layer Stress Difference

After fracturing, the gas and water production dynamics of gas wells are similar, showing the characteristics of rapid rise of production at first, then rapid decline, and finally being stable. Its full life cycle can be divided into three stages: ① rapid production stage, ② production decline stage, and ③ steady production stage (Fig. 10). The provenance of rapid production stage is mainly from hydraulic fractures. Artificial fractures formed after fracturing have high porosity and high permeability, which is a good storage and permeability space. Fluids stored in hydraulic fractures can flow rapidly to the bottom of the well through the hyper-permeability channel. This stage is limited by the fracture volume and lasts for a short time. The pressure drop in the production decline stage is transmitted to the reservoir matrix, and due to the physical properties of the matrix, it is difficult to timely supplement the fracture pressure drop in the production process, resulting in the phenomenon of sharp reduction of productivity. The productivity decline rate and the duration of this stage are related to the difference in the physical properties of the fracture and reservoir matrix. The source of the stable production stage comes from the

reservoir matrix, and at this time, the reservoir matrix, hydraulic fracture and bottom hole form a relatively stable pressure drop. The productivity of this stage is jointly determined by the size of hydraulic fracture and reservoir physical property.

By comparing the gas and water production dynamics under different inter-layer stress difference conditions (Fig. 10), it can be seen that with the increase of inter-layer stress difference, the hydraulic fracture length increases, while the dimensionless reservoir reconstruction volume coefficient decreases, and the gas well production decreases significantly with the decrease of fracturing reconstruction volume. There is only a slight difference in water production between the end of the first stage and the end of the second stage. The larger the fracturing volume is, the greater the corresponding water production in these two stages is. The reservoir does not develop boundless bottom water and distinct water layer, therefore the gap of water production under different conditions is small.

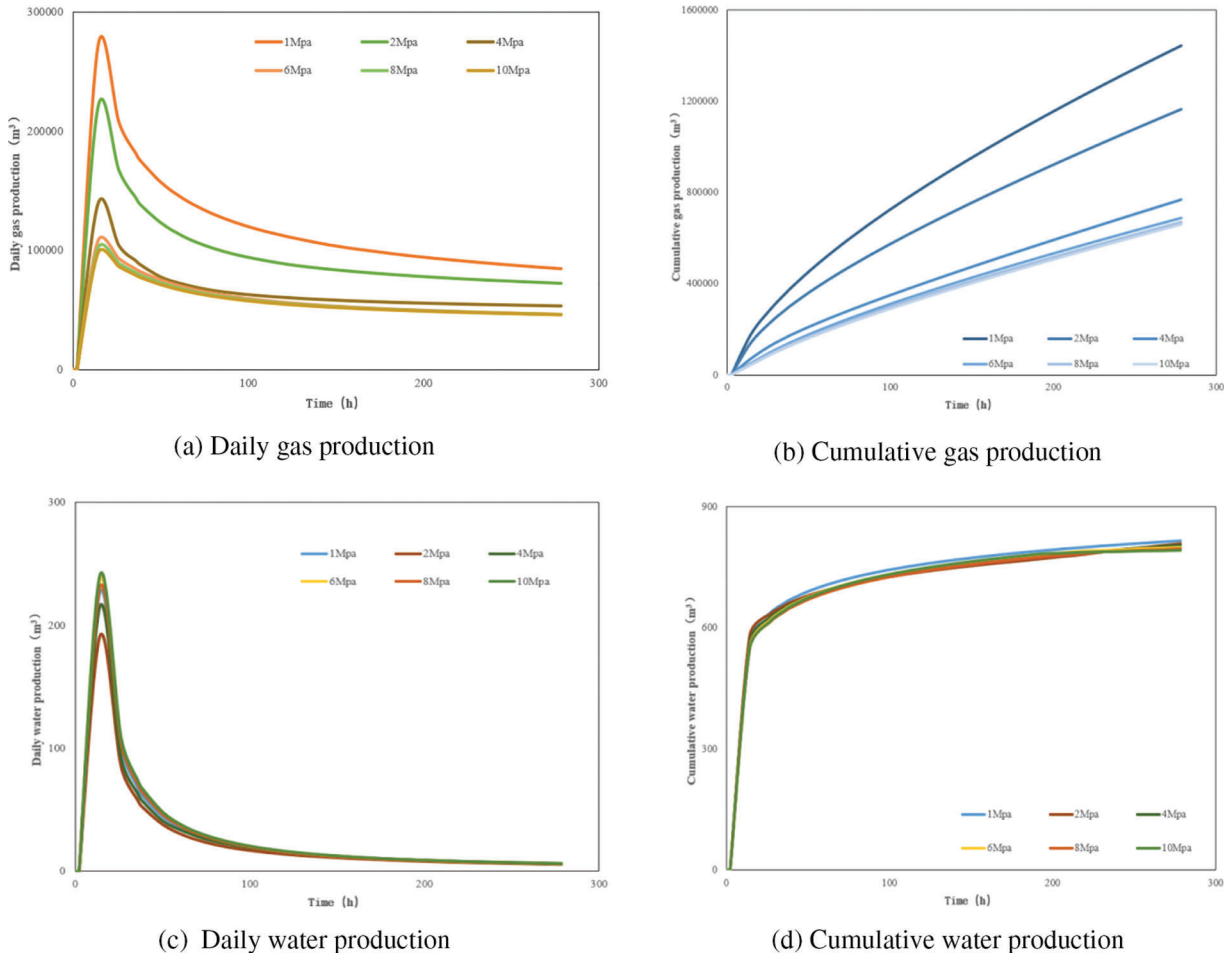

(a) Daily gas production

(b) Cumulative gas production

(c) Daily water production

(d) Cumulative water production

Figure 10: Gas and water production under different inter-layer stress difference conditions

6.2 Fracturing Construction Displacement

Fig. 11 shows the gas and water production dynamic curves under different fracturing construction displacement conditions. It can be compared and seen that with the increase of fracturing construction displacement and fracture size, dimensionless reconstruction volume coefficient also increase. Gas and water production and fracturing construction displacement of gas well present a positive correlation. Due

to tight reservoir, water production is of small difference and maintained at a low level after fracturing fluid flow-back under the condition.

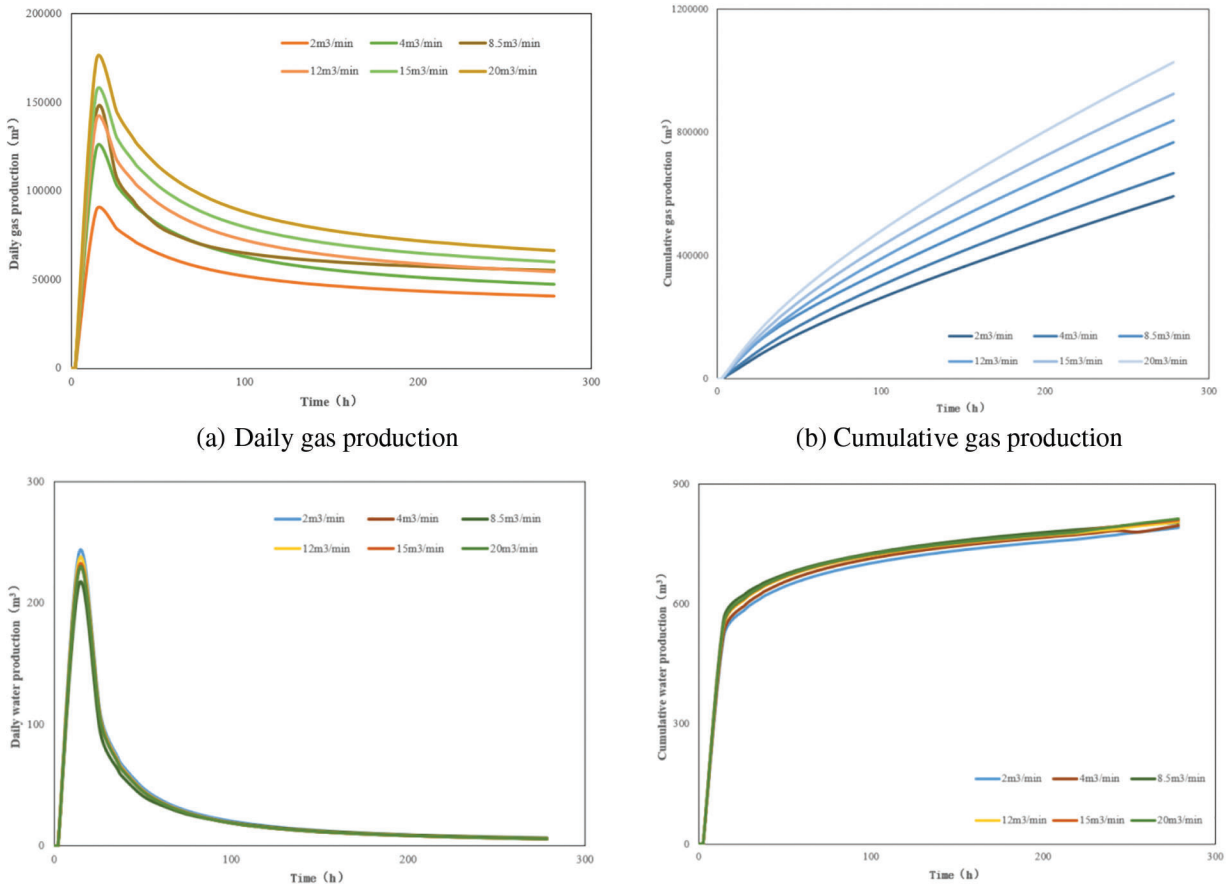

(a) Daily gas production

(b) Cumulative gas production

(c) Daily water production

(d) Cumulative water production

Figure 11: Gas and water production dynamics under different fracturing construction displacement conditions

6.3 Fracturing Fluid Viscosity

By comparing the fracture size, dimensionless reconstruction volume and gas water production dynamics under different fracturing fluid viscosities (Fig. 12), it can be seen that the gas production capacity of the gas well is divided into two stages. The hydraulic fractures generated by high-viscosity fracturing fluid are characterized by short, wide and high length. They have good physical properties, sufficient initial provenance, short seepage distance and high production. Under the same dimensionless reconstruction volume condition, the controllable reserves of long fractures generated by low viscosity fracturing fluid are larger and the later production is higher. There is little difference in water production under different conditions. Although there is no difference in fracture volume due to non-dimensional reconstruction in the late of first stage, the difference gradually decreases with the progress of production and eventually tends to be consistent.

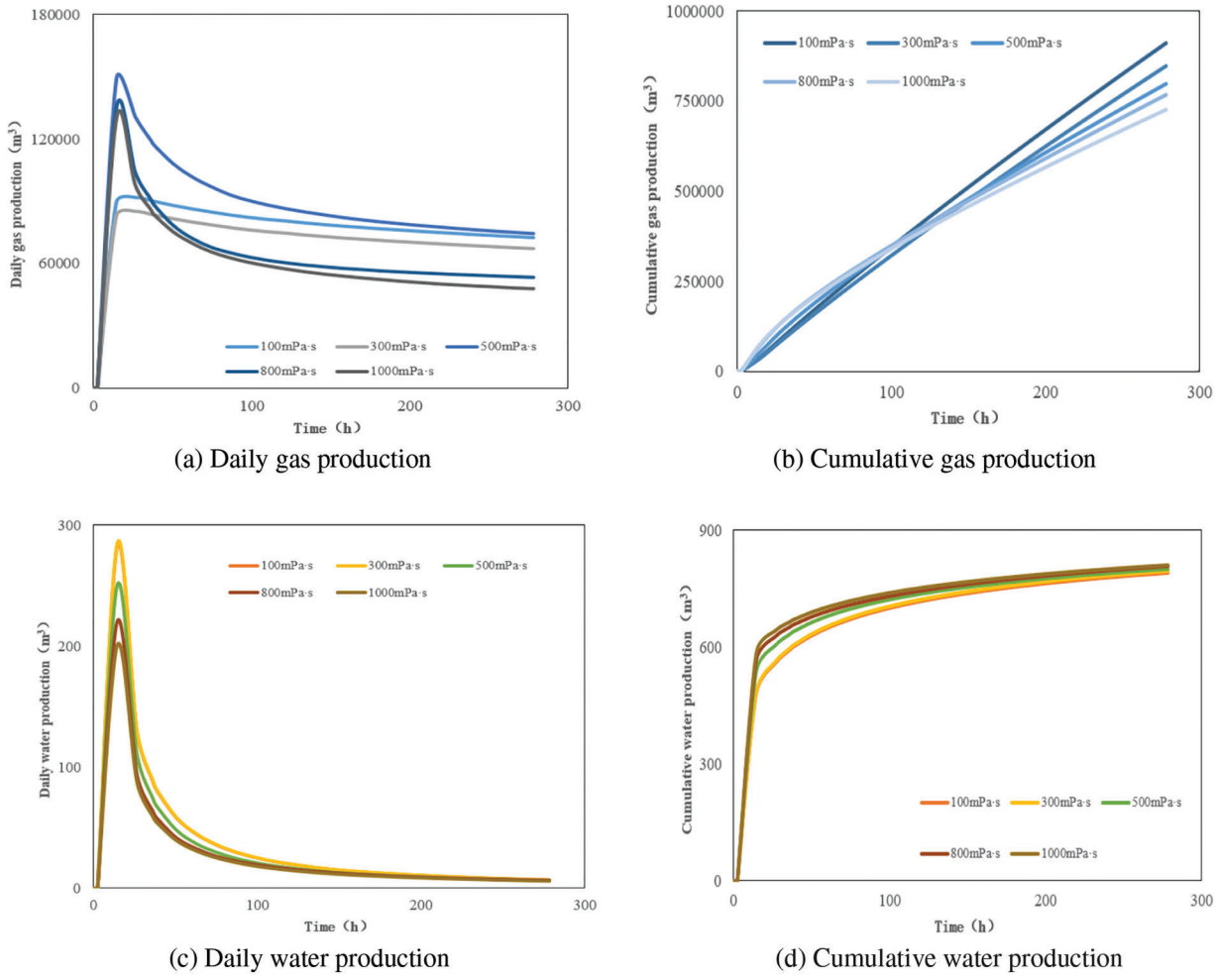

(a) Daily gas production (b) Cumulative gas production

(c) Daily water production (d) Cumulative water production

Figure 12: Gas-water production dynamics under different fracturing fluid viscosity conditions

7 Conclusion

1) The inter-layer stress difference can effectively control the joint height and promote the development of joint length. Large displacement fracturing is conducive to improving the efficiency of fracture formation and expanding the fracture size. Low viscosity fracturing fluid is suitable for making long fractures, while high viscosity fracturing fluid is suitable for making wide fractures. The dimensionless reconstruction volume of reservoir has a negative correlation with inter-layer stress difference and a positive correlation with the fracturing displacement. It increases first and then decreases with the increase of fracturing fluid viscosity. The dimensionless reconstruction volume of reservoir has a small difference under different fracturing fluid viscosity.

2) The flow-back rate is mainly determined by the physical properties of the reservoir and the properties of the fracturing fluid. Under different influencing factors, the flow-back rate after pressure is highly correlated with the dimensionless reconstruction volume of the reservoir. The lower the fracturing fluid reservoir intrusion, the higher the fracture formation efficiency, and the larger the dimensionless reconstruction volume, the higher the fracturing fluid flow-back rate. What's more, rapid flow-back can effectively reduce fracturing fluid reservoir intrusion and improve reservoir flow-back efficiency.

3) Gas well production can be divided into three stages. The production in the first stage is determined by dimensionless reservoir reconstruction volume; the production in the second stage is determined by dimensionless reservoir reconstruction volume and reservoir physical property; and the production in the third stage is determined by reservoir physical property. The smaller the inter-layer stress difference is as well as the larger the fracturing displacement is, the larger the dimensionless reservoir reconstruction volume is and the higher the gas production is. What's more, the higher the viscosity of the fracturing fluid and the lower the gas production in the case of similar dimensionless reservoir reconstruction volume, the longer the fracture length is, the higher the third-stage production and the final production are.

4) In the case of boundless bottom water or clear water layer, the water production of fractures with different sizes has little difference. The influence of different factors on the water production of gas wells is mainly reflected in the first production stage. The larger the dimensionless reconstruction volume of the reservoir, the larger the water production in the initial production stage, and eventually tends to be consistent with the progress of production time.

Acknowledgement: None.

Funding Statement: The authors received no specific funding for this study.

Author Contributions: The authors confirm contribution to the paper as follows: study conception and design: Yan Liu and Tianli Sun; data collection: Bencheng Wang; numerical simulation: Yan Feng; analysis and interpretation of results: Yan Liu, Tianli Sun and Yan Feng; draft manuscript preparation: Bencheng Wang and Yan Feng. All authors reviewed the results and approved the final version of the manuscript.

Availability of Data and Materials: The authors confirm that the data supporting the findings of this study are available within the article.

Conflicts of Interest: The authors declare that they have no conflicts of interest to report regarding the present study.

References

1. U. S. Energy Information Administration (2019). U. S. natural gas exports and re-exports by country. https://www.eia.gov/dnav/ng/ng_move_expc_s1_a.htm (accessed on 07/11/2019).
2. Boak, J., Kleinberg, R. (2020). Shale gas, tight oil, shale oil and hydraulic fracturing. In: Trevor, M. (Ed.), *Future Energy*, pp. 67–95. Elsevier, The Netherlands: Amsterdam.
3. Ahmed, U., Meehan, D. N. (2016). *Unconventional oil and gas resources: Exploitation and development*, 1st edition. Boca Raton, Florida: Taylor & Francis.
4. Syed, F. I., Dahaghi, A. K., Muther, T. (2022). Laboratory to field scale assessment for EOR applicability in tight oil reservoir. *Petrol Science, 19(5),* 2131–2149.
5. Guo, W., Pan, J. P. (2019). Mid-term evaluation and prospect of the implementation of the 13th Five-Year Plan for the national oil and gas resources exploration and mining plan. *The Natural Gas Industry, 39(4),* 111–117.
6. Wang, Y. F. (2021). The exploration and development prospects of unconventional oil and gas resources in China are broad. *Prospect Develop, 1(6),* 14–15.
7. Qiu, Z., Zou, C. N. (2020). Unconventional oil and gas sedimentology: Connotation and prospects. *Acta Sedimentologica Sinica, 38(1),* 1–29.
8. Fu, H. F., Cai, B., Geng, M., Jia, A. L., Weng, D. W. et al. (2022). Three dimensional simulation of hydraulic fracture propagation based on vertical reservoir heterogeneity. *Natural Gas Industry, 42(5),* 56–68.

9. Peng, Y., Zhao, J. Z., Sepehrnoori, K., Li, Z., Xu, F. (2019). Study of delayed creep fracture initiation and propagation based on semi-analytical fractional model. *Applied Mathematical Modelling, 72,* 700–715. https://doi.org/10.1016/j.apm.2019.03.034
10. Zhang, D. W., Yang, Y. (2022). Exploration potential and development direction of continental tight sandstone gas in the Sichuan Basin. *Natural Gas Industry, 42(1),* 1–11.
11. Zou, C. N., Pan, S. Q., Zhao, Q. (2020). On the connotation, challenge and significance of China'senergy independence strategy. *Petroleum Exploration and Development, 47(2),* 416–426.
12. Dou, L. R., Wen, Z. X., Wang, J. J., Wang, Z. M., He, Z. J. et al. (2022). Analysis of the world oil and gas exploration situation in 2021. *Petroleum Exploration and Development, 49(5),* 1033–1044.
13. Liu, Z. Q. (2022). New progress in development technology for difficult to produce reserves in deep tight sandstone gas reservoirs of the Xujiahe formation in the Sichuan Basin. *Oil & Gas Geology, 43(5),* 1010.
14. Liu, Z. Q., Xu, S. L., Liu, J. L., Ma, L. Y., Liu, S. B. et al. (2020). Enrichment laws of deep tight sandstone gas reservoirs in the Western Sichuan Depression, Sichuan Basin. *Natural Gas Industry, 40(2),* 31–40.
15. Zhao, Z. W., Tang, D. H., Wang, X. J., Chen, S. L. (2019). Discussion on main controlling factors of natural gas enrichment and high yield in tight sandstone gas reservoirs: Case study of Xujiahe Formation in Sichuan Basin. *Natural Gas Geoscience, 30(7),* 963–972.
16. Zheng, H. R., Liu, Z. Q., Xu, S. L., Liu, Z. F., Liu, J. L. et al. (2021). Progress and key research directions of tight gas exploration and development in Xujiahe Formation, Sinopec exploration areas, Sichuan Basin. *Oil & Gas Geology, 42(4),* 765–783.
17. Liu, Z. Q., Luo, K. P., Tang, Y., Yang, F., Mei, L. F. et al. (2019). Critical tectonic periods and the response of gas accumulation in non marine tight sandstone reservoir in Yuanba-Tongnanba Area, Sichuan Basin. *Earth Science, 44(3),* 756–772.
18. Cao, Y. C., Qian, K. L., Liu, K. Y., Zhu, R. K., Yuan, G. H. et al. (2018). Reservoir properties characterization and its genetic mechanism for tight sandstone oil and gas reservoir in lacustrine basin: The case of the fourth member of lower cretaceous quantou formation in the Southern Songliao Basin. *Acta Petrolei Sinica, 39(3),* 247–265.
19. Economides, M. J., Martin, T. (2018). *Modern fracturing: Enhancing natural gas production*, lst edition. Houston: ET Publishing.
20. Asadi, M., Scharmach, W., Jones, T., Sampayo, A., Chesney, E. et al. (2015). Water-free fracturing: A case history. *Proceedings of the SPE/CSUR Unconventional Resources Conference*,, *Calgary, Alberta, Canada*.
21. Wan, Y. Y., Zhang, Y. X., Zhang, L., Liu, Y., Xie, G. Q. (2021). Research and application of crack height control fracturing echnology in thin interbeds with low stress difference. *Technology Supervision in Petroleum Industry, 37(1),* 57–60.
22. Wei, G. Q., Zhang, F. D., Li, J., Yang, S., Huang, C. Y. et al. (2016). New progress of tight sand gas accumulation theory and favorable exploration zones in China. *Natural Gas Geoscience, 27(2),* 199–210.
23. Ostojic, J., Rezaee, R., Bahrami, H. (2012). Production performance of hydraulic fractures in tight gas sands, a numerical simulation approach. *Journal of Petroleum Science and Engineering, 88–89,* 75–81. https://doi.org/10.1016/j.petrol.2011.11.002
24. Medavarapu, K., Das, S., Ch, S., Nainwal, S. P. (2017). Optimization of fracturing technique for successful exploitation of tight gas reservoirs of Mandapeta field. *SPE Oil and Gas India Conference and Exhibition*, *Mumbai, India*. https://doi.org/10.2118/185421-MS
25. Liu, P. G., Du, S. H., Hou, F. (2020). Quantitative characterization of fracturing effect of tight reservoir based on full-length fracturing simulation technology. *Journal of China University of Petroleum (Edition of Natural Science), 44(5),* 10–18 (In Chinese).
26. Qu, Z. Q., Tian, Y., Li, J. X., Guo, T. K., Li, X. L. et al. (2017). Numerical simulation study on fracture extension and morphology of multi-cluster staged fracturing for horizontal wells. *Journal of China University of Petroleum (Edition of Natural Science), 41(1),* 102–109 (In Chinese).
27. Li, Y. M., Peng, Y., Zhao, J. Z., Sepehrnoori, K., Yang, Y. (2018). An improved fracture height containment method: Artificial gel-barrier technology and its simulation. *Environmental Earth Sciences, 77,* 324. https://doi.org/10.1007/s12665-018-7506-3

28. Ye, L., Li, X. W., Ma, X. X., Li, S. H., Zhao, Q. Y. et al. (2020). Experiments on hydraulic fracture propagation in tight sandstones with different brittleness. *Xinjiang Petroleum Geology, 41(5),* 575–581.
29. Flewelling, S. A., Tymchak, M. P., Warpinski, N. (2013). Hydraulic fracture height limits and fault interactions in tight oil and gas formations. *Geophysical Research Letters, 40(14),* 3602–3606. https://doi.org/10.1002/grl.v40.14
30. Jeffrey, R. G., Bunger, A. P. (2007). A detailed comparison of experimental and numerical data on hydraulic fracture height growth through stress contrasts. *SPE Journal, 14(3),* 413–422.
31. Ishida, T., Chen, Q., Mizuta, Y., Roegiers, J. C. (2004). Influence of fluid viscosity on the hydraulic fracturing mechanism. *Journal of Energy Resources Technology, 126(3),* 190–200. https://doi.org/10.1115/1.1791651
32. Li, J. (2022). *Investigation on fracture geometry of continental tight sandstone from Northeast Sichuan in true triaxial hydraulic fracturing test under different pumping rates (Master Thesis)*. North China University of Water Resources and Electric Power, Zhengzhou, China.
33. Muther, T., Nizamani, A. A., Ismail, A. R. (2020). Analysis on the effect of different fracture geometries on the productivity of tight gas reservoirs. *Malaysian Journal of Fundamental and Applied Sciences, 16(2),* 201–211. https://doi.org/10.11113/mjfas.v16n2.1343
34. Zhao, J. Z., Peng, Y., Li, Y. M., Xiao, W. L. (2015). Analytical model for simulating and analyzing the influence of interfacial slip on fracture height propagation in shale gas layers. *Environmental Earth Sciences, 73(10),* 5867–5875. https://doi.org/10.1007/s12665-015-4360-4
35. Zhao, J. Z., Peng, Y., Li, Y. M., Tian, Z. S. (2015). Applicable conditions and analytical corrections of plane strain assumption in the simulation of hydraulic fracturing. *Petroleum Exploration and Development, 44(3),* 454–461.
36. Wang, R., Song, H., Tang, H., Wang, Y., Killough, J. et al. (2016). Analytical modeling of gas production rate in tight channel sandformation and optimization of artificial fracture. *Springer Plus, 5,* 540. https://doi.org/10.1186/s40064-016-2176-7
37. Huang, Y. Q., Xiao, K. H., Jin, W. J., Wang, A., Liu, Z. Y. et al. (2023). Characteristics and controlling factors of tight sandstone reservoir fractures in the Xujiahe formation of the western Yuanba area northeastern Sichuan Basin. *Bulletin of Geological Science and Technology, 42(2),* 105–114.
38. Wang, A., Zhong, D. K., Liu, Z. Q., Wang, W., Du, H. Q. et al. (2022). Characteristics of deep tight sandstone reservoirs and their controlling factors of physical properties: A case study of the Xu-2 member in the western Yuanba area of the Northeastern Sichuan Basin China. *Acta Sedimentologica Sinica, 40(2),* 410–421.
39. Tang, J. R., Wang, J. Y., Zhang, C. C., Song, G. Z., Shi, Y. T. et al. (2015). Sedimentary characteristics and their relationship with tight sandstone gas within the source rock of tight gas: A case study from third member of Xujiahe formation in Yuanba area, NE Sichuan Basin. *Acta Sedimentologica Sinica, 33(6),* 1224–1234.
40. Sun, H. T., Zhong, D. K., Wang, W., Wang, A., Yang, S. et al. (2021). Origin analysis of a tight sandstone reservoir for the Xujiahe formation of the upper triassic at the Malubei Area in the Sichuan Basin, China. *Acta Sedimentologica Sinica, 39(5),* 1057–1067.
41. Jiang, Y. L., Li, M. Y., Wang, L. J., Liu, J. D., Zeng, T. et al. (2020). Characteristics and controlling factors of tight sandstone reservoir fractures of the Xuj iahe formation in the Bazhong-Tongnanba area, Northeast Sichuan. *Acta Geologica Sinica, 94(5),* 1525–1537.
42. Yao, L. (2012). *Tight sandstone reservoir characteristics of upper triassic Xujiahe formation in the Puguang area (Master Thesis)*. Yangtze University, Jingzhou, China.
43. King, G. E., Haile, L., Shuss, J., Dobkins, T. (2008). Increasing fracture path complexity and controlling downward fracture growth in the Barnett shale. *SPE Shale Gas Production Conference*, Fort Worth, Texas, USA.
44. Meyer & Associates, Inc. (2010). *Meyer fracturing simulators user's guide*. Eighth Edition. Texas, USA.
45. Mever, B. R. (1986). Design formulae for 2-D and 3-D vertical hydraulic fractures: Model comparison and parametric studies. *SPE Unconventional Gas Technology Symposium*, Louisville, KY, China.
46. Ramurthy, M., Barree, R. D., Broacha, E., Longwell, J. D., Kundert, D. P. et al. (2009). Effects of high process-zone stress in shale stimulation treatments. *SPE Rocky Mountain Petroleum Technology Conference*, Denver, Colorado, USA. https://doi.org/10.2118/123581-MS

47. Huang, C. H., Zhu, H. Y., Wang, J. D., Han, J., Zhou, G. O. et al. (2022). A FEM-DFN model for theinteraction and propagation of multi-cluster fractures during variablefluid-viscosity injection in layered shale oil reservoir. *Petroleum Science, 19(6),* 2796–2809. https://doi.org/10.1016/j.petsci.2022.06.007
48. Xu, W., Thiercelin, M. J., Ganguly, U., Weng, X., Gu, H. (2010). Wiremesh: A novel shale fracturing simulator. *International oil and gas conference and exhibition in China*. Beijing, China, Society of Petroleum Engineers.
49. Meyer, B. R., Bazan, L. W. (2011). A discrete fracture network model for hydraulically induced fractures-theory, parametric and case studies. *SPE Hydraulic Fracturing Technology Conference*, Woodlands, Texas, Society of Petroleum Engineers.
50. Li, Z. L., Duan, Y. G., Peng, Y., Wei, M. Q., Wang, R. (2020). A laboratory study of microcracks variations in shale induced by temperature change. *Fuel, 280,* 118636. https://doi.org/10.1016/j.fuel.2020.118636
51. Li, Y. M., Liao, Y., Zhao, J. Z., Peng, Y., Pu, X. (2017). Simulation and analysis of wormhole formation in carbonate rocks considering heat transmission process. *Journal of Natural Gas Science and Engineering, 42,* 120–132. https://doi.org/10.1016/j.jngse.2017.02.048